

TITAN'S GLOBAL MAP COMBINING VIMS AND ISS MOSAICS. B. Seignovet^{1,2}, S. Le Mouélic², R. H. Brown³, E. Karkoschka³, V. Pasek³, C. Sotin¹ and E. P. Turtle⁴, ¹Jet Propulsion Laboratory, California Institute of Technology, Pasadena, CA, USA, ²LPG, UMR 6112, CNRS, Université de Nantes, 2 rue de la Houssinière, Nantes, France, ³Department of Planetary Sciences, University of Arizona, Tucson, AZ, USA, ⁴Johns Hopkins Applied Physics Laboratory, Laurel, MD, USA.

Introduction: Titan, Saturn's largest moon, is the only ocean world, besides Earth, with a dense atmosphere. This outstanding feature is also a challenge since it was believed before the launch of the Cassini mission that optical cameras (visible and infrared) could not see the surface and that only radar instruments could map Titan's surface. However, the Visual and Infrared Mapping Spectrometer (VIMS) and the Imaging Science Subsystem (ISS) onboard the Cassini spacecraft demonstrated that Titan's surface can be observed in several infrared atmospheric windows. These windows are located at (1.08, 1.27, 1.59, 2.03, 2.69, 2.78 and 5 μm) for VIMS [1, 2] and 938 nm for ISS [3]. Between 2004 and 2017, Cassini performed 127 targeted Titan flybys and recorded about 60,000 VIMS hyperspectral cubes [4] and 20,000 ISS images at 938 nm using the CB3 filter [5].

Both datasets were acquired with a variety of observing geometries (incidence, emission, and phase angles) and different atmospheric characteristics. Light scattered by aerosols complicates the radiative transfer model to infer surface albedo. The VIMS observations are small hyperspectral images of 64 pixels \times 64 pixels spanning a large range in pixel size from 500 m to 30 km. 90 % of Titan's surface is covered by VIMS images at better than 25 km/pixel and only 5 % at better than 5 km/pixel [4]. The ISS images are 1024 pixels \times 1024 pixels with typically a few kilometers pixel scale, and provide a more homogeneous global coverage. Semi-empirical techniques have been used but seams have proven to be extremely difficult to remove [6, 7] (Fig. 1a,b).

This study combines the VIMS color mosaics at different wavelengths [4] and the global ISS mosaic [5] to provide a seam-free color map of Titan revealing the diversity of geological structures.

Method: We selected the VIMS map in band ratio at 1.59/1.27 (red), 2.03/1.27 (green) and 1.27/1.08 μm (blue) from [4]. This map provides the highest sensitivity to the surface composition and highlights its variability. The equatorial dunes fields appear in brownish tones, and several occurrences of bluish tones are localized in areas such as Sinlap, Menrva and Selk craters. However, some regions are not covered (80°S, 120°E) or are affected by extreme observation geometries. The saturated yellow area at (70°N, 40°E) is due to a specular reflection on Kraken Mare.

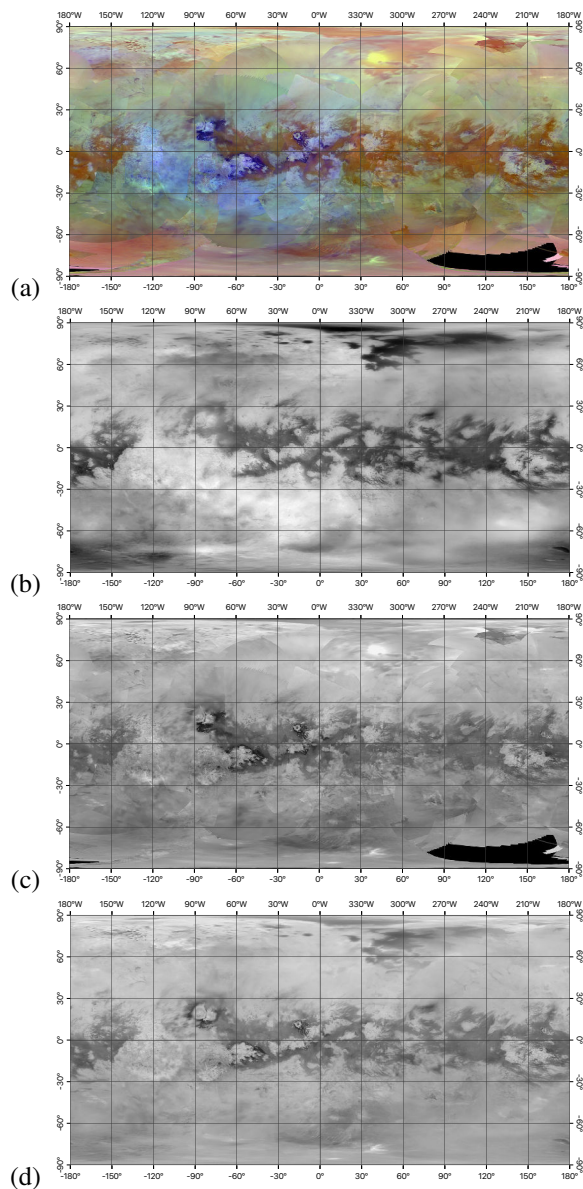


Figure 1: (a) VIMS RGB global map at 1.59/1.27, 2.03/1.27 and 1.27/1.08 μm empirically corrected for airmass effects [4]. (b) ISS grayscale global map at 938 nm [5]. (c) Original L^* lightness component of VIMS map. (d) Combined VIMS L^* component with filtered ISS map.

To keep the spectral information from VIMS we decompose the representative RGB map into three

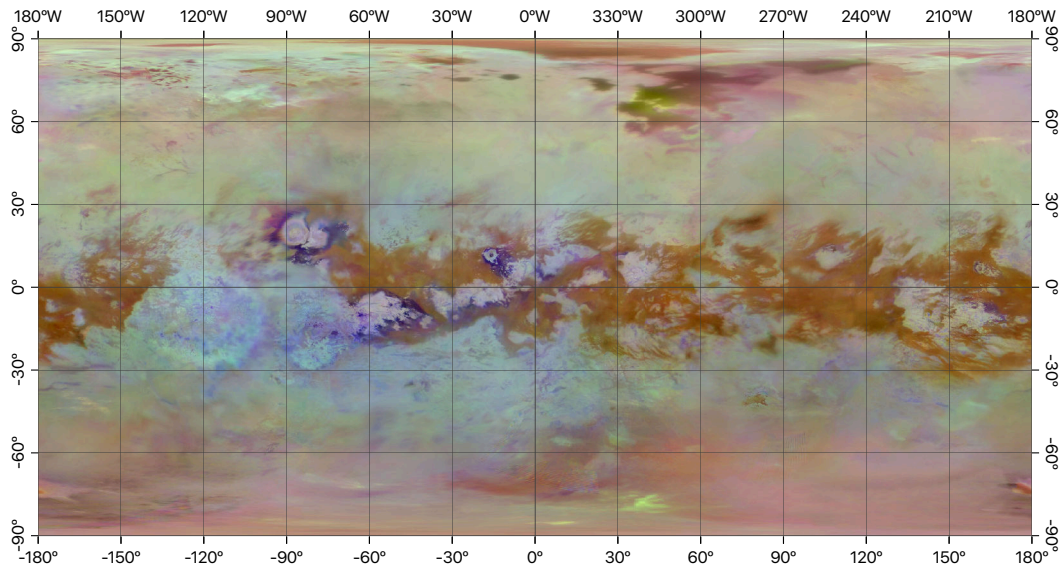


Figure 2: Combined VIMS and ISS global map in equirectangular projection.

channels: lightness (L^*), the green–red (a^*) and blue–yellow (b^*) color components (CIELAB decomposition from [8]). The VIMS L^* component (Fig. 1c) looks similar to the albedo map retrieved by ISS (Fig. 1b).

In order to better emphasize the north-polar lakes and seas and the equatorial features from ISS, we added the ISS albedo map to L^* with a darkening luminosity filter of 50 % to extract the details from the darkest areas of the ISS map. Additionally, we use the VIMS resolution map (Fig. 1 from [4]) – smoothed with a Gaussian filter of 15 pixels radius to remove the seams between the different cubes – as a secondary filter to preserve the high resolution area covered by VIMS (Fig 1d). Where VIMS data don't exist, the value of a^* and b^* components are filled with the mean value of the adjacent pixels and the remaining seams are manually removed. Finally, the new lightness layer is recombined with the filled a^* and b^* layers to compose a new color map (Fig. 2).

Discussion: Merging the two data sets is a real challenge. The coregistration of the two global maps is accurate to a few kilometers. Locally, some advanced refinements could be required but the overall correlation matches the expected resolution provided by the instruments.

Compared to the original VIMS map, the contours of the northern maria and lakes are more pronounced and can be individually identified. The specular reflection over Kraken Mare is partly compensated by the ISS data. In the equatorial region, the high resolution VIMS data over the craters Sinlap, Menrva and Selk are preserved and the sharpness of the dune fields

is increased. The light blue feature centered at (10°S, 120°W) within Xanadu was already present in the original VIMS map [9]. Finally, at the South Pole, the gap at (80°S, 120°E) is now covered but its spectral interpretation is unknown due to the absence of VIMS data. The western part of Ontario Lacus is also completed by the ISS map.

This combined VIMS-ISS map provides an overview of Titan's known geological features. The differences in color reflect differences in geomorphology and composition (e.g. the equatorial dune field [10] appears in brownish tones whereas the dark blue areas are interpreted as local enrichment in water ice [11]). This map could be used as a basemap for local studies but feature identification is best conducted using the original VIMS [4] and ISS [5] maps.

Acknowledgments: This work has been partly performed at the Jet Propulsion Laboratory, California Institute of Technology, under contract to NASA. CNES support is acknowledged.

References: [1] Brown R. H. et al. (2004) *The Cassini-Huygens Mission*, 111–168. [2] Sotin C. et al. (2005) *Nature*, 435:786–789. [3] Porco C. C. et al. (2004) *Space Sci. Rev.*, 115:363–497. [4] Le Mouélic S. et al. (2019) *Icarus*, 319:121–132. [5] Karkoschka E. et al. (2017) *LPSC #2518*. [6] Le Mouélic S. et al. (2012) *PSS*, 73:178–190. [7] Turtle E. P. et al. (2009) *GRL*, 36(2). [8] Robertson A. R. (1977) *Color Research & Application*, 2:7–11. [9] Brown R. H. et al. (2011) *Icarus*, 214:556–560. [10] Brossier J. F. et al. (2018) *JGR*, 123:1089–1112. [11] Solomonidou A. et al. (2018) *JGR*, 123:489–507.